

# NASA ExoPAG Study Analysis Group 11: Preparing for the WFIRST Microlensing Survey

Jennifer C. Yee<sup>1</sup> (chair), Michael Albrow<sup>2</sup>, Richard K. Barry<sup>3</sup>, David Bennett<sup>4</sup>, Geoff Bryden<sup>5</sup>, Sun-Ju Chung<sup>6</sup>, B. Scott Gaudi<sup>7</sup>, Neil Gehrels<sup>3</sup>, Andrew Gould<sup>7</sup>, Matthew T. Penny<sup>7</sup>, Nicholas Rattenbury<sup>8</sup>, Yoon-Hyun Ryu<sup>6,9</sup>, Jan Skowron<sup>10</sup>, Rachel Street<sup>11</sup>, Takahiro Sumi<sup>12</sup>

<sup>1</sup> Sagan Fellow, Harvard-Smithsonian Center for Astrophysics, 60 Garden St., Cambridge, MA 02138, USA

<sup>2</sup> Department of Physics and Astronomy, University of Canterbury, Private Bag 4800, Christchurch, New Zealand

<sup>3</sup> Astrophysics Science Division, NASA Goddard Space Flight Center, Greenbelt, MD 20771, USA

<sup>4</sup> University of Notre Dame, Department of Physics, 225 Nieuwland Science Hall, Notre Dame, IN 46556-5670, USA

<sup>5</sup> Jet Propulsion Laboratory, M/S 169-506, 4800 Oak Grove Drive, Pasadena, CA, 91109, USA

<sup>6</sup> Korea Astronomy and Space Science Institute, Hwaam-Dong, Yuseong-Gu, Daejeon 305-348, Republic of Korea

<sup>7</sup> Department of Astronomy, Ohio State University, 140 West 18th Avenue, Columbus, OH 43210, USA

<sup>8</sup> Department of Physics, University of Auckland, Private Bag 92-019, Auckland 1001, New Zealand

<sup>9</sup> Department of Astronomy and Atmospheric Sciences, Kyungpook National University, Daegu 702-701, Republic of Korea

<sup>10</sup> Warsaw University Observatory, Al. Ujazdowskie 4, 00-478 Warszawa, Poland

<sup>11</sup> Las Cumbres Observatory Global Telescope Network, 6740 Cortona Drive, Suite 102, Goleta, CA 93117, USA

<sup>12</sup> Department of Earth and Space Science, Osaka University, Osaka 560-0043, Japan

July 31, 2018

## Executive Summary

The *WFIRST* microlensing survey will observe tens of thousands of microlensing events and detect thousands of planets, including free-floating planets. Because of its high resolution and high photometric accuracy, *WFIRST* will characterize these events at an unprecedented level of precision. It will be able to routinely observe higher-order microlensing effects, which can be combined in various ways to yield masses for the lens (host) stars and therefore the true masses of the planets (rather than just the mass ratio  $q = m_p/M_{\text{star}}$ ). In addition, because this survey will be performed in the near-IR, *WFIRST* will be able to observe extincted parts of the Galactic bulge not covered by optical microlensing surveys, and because it is in space, *WFIRST* will reach magnitudes far fainter than can be achieved from the ground. However, because *WFIRST* will far exceed the capabilities of ground-based microlensing surveys, the exact potential of these new opportunities is unknown. **We identify the following programs that will enhance *WFIRST* microlensing science and reduce the mission’s scientific risk.**

### 1. Precursor *HST* Observations

The *WFIRST* microlensing survey will be the first survey capable of systematically measuring the astrometric microlensing effect, which gives a measurement of the angular size of the Einstein ring,  $\theta_E$ , and the relative proper motion between the source and the lens. Measuring these effects is vital for measuring lens masses with *WFIRST*. They can be combined with other effects to measure masses even for planets with faint host stars (e.g., brown dwarfs) and for planets detected without caustic crossings. However, most astrometric microlensing signals will be close to the signal-to-noise ratio limit, and because this effect is so difficult to measure without *WFIRST*-like capabilities, the systematics are unknown.

**The best way to validate the *WFIRST* astrometric microlensing measurements is to conduct precursor *HST* imaging of the *WFIRST* field  $\sim 10$  years in advance.** Optical, single-epoch, imaging of the field at this time will resolve 20% of the lenses and sources that will be future *WFIRST* microlensing events. The observed *HST* separation gives a direct measurement of the source-lens relative proper motion for comparison with the astrometric microlensing results. In addition, these proper motion measurements can be used to calculate  $\theta_E$  for events without observable finite source or astrometric microlensing effects.

In addition, **multi-epoch observations of a few fields using *HST*/WFC3/IR will provide a valuable data set for testing the *WFIRST* photometry/astrometry pipeline, the development of which is mission-critical.**

## 2. A Ground-Based, Near-IR, Microlensing Survey

The near-IR microlensing event rate in the potential *WFIRST* fields has never been measured. Much of our current understanding of these fields comes from extrapolations of optical microlensing surveys both to redder wavelengths and lower Galactic latitude. Improving our understanding of these fields is crucial both for reducing scientific risk from uncertainties in the simulations of the *WFIRST* mission and for optimizing the microlensing field to maximize *WFIRST*'s scientific return. **The best way to characterize the *WFIRST* field is to conduct a near-IR microlensing survey from the ground.** This will provide a direct measurement of the microlensing event rate for bright stars and a preliminary understanding of the source luminosity function. Thus, it will reduce scientific risk for *WFIRST* by improving our simulations and predictions for the *WFIRST* planet yield.

## 3. Development of Expertise

There are also several other programs that will support *WFIRST* science. **Projects to measure parallax (e.g., with *Spitzer* or *Kepler*), astrometric microlensing, and lens fluxes with current instrumentation will all help to develop the techniques that *WFIRST* will use to measure lens masses while providing preliminary data on the relative populations of planets in the disk and the bulge.** In addition, a competition in microlensing analysis could stimulate the development of new techniques to handle the vast microlensing data set that *WFIRST* will produce.

## Contents

<b>Executive Summary</b>	<b>1</b>
<b>1 Introduction</b>	<b>5</b>
1.1 <i>WFIRST</i> Planet Masses . . . . .	6
1.2 Field Selection . . . . .	6
1.3 Microlensing Techniques . . . . .	7
<b>2 Optical <i>HST</i> Imaging of the <i>WFIRST</i> fields</b>	<b>8</b>
2.1 Astrometric Microlensing . . . . .	8
2.2 Program Description . . . . .	9
2.3 Additional <i>WFIRST</i> Microlensing Science . . . . .	10
2.4 Other Science . . . . .	11
<b>3 Ground-based, Near-IR, Microlensing Survey</b>	<b>11</b>
3.1 Unknown Event Rate in the <i>WFIRST</i> Field . . . . .	11
3.2 Description of the Survey . . . . .	12
3.3 <i>WFIRST</i> Science Outcomes . . . . .	12
3.4 Other Science . . . . .	13
<b>4 Satellite Parallaxes</b>	<b>13</b>
4.1 Microlensing Satellite Parallax . . . . .	13
4.2 <i>Spitzer</i> parallaxes . . . . .	14
4.3 <i>Kepler</i> parallaxes . . . . .	14
4.4 <i>TESS</i> parallaxes . . . . .	16
4.5 Direct Relevance to <i>WFIRST</i> . . . . .	16
<b>5 Lens Flux Measurements of Current Microlensing Events</b>	<b>17</b>
5.1 Detecting Light from the Lenses . . . . .	17
5.2 Current Capabilities . . . . .	18

<b>6</b>	<b>Astrometric Microlensing Due to Black Holes</b>	<b>18</b>
<b>7</b>	<b>Multi-Epoch, Near-IR, <i>HST</i> Observations</b>	<b>19</b>
<b>8</b>	<b>Microlensing Analysis Challenge</b>	<b>19</b>
8.1	Complexities in Microlensing Analysis . . . . .	19
8.2	Parameters of the Challenge . . . . .	20
<b>9</b>	<b>Conclusions</b>	<b>21</b>
<b>A</b>	<b>Appendix: Charter</b>	<b>23</b>
<b>B</b>	<b>Appendix: Introduction to <i>WFIRST</i> Microlensing</b>	<b>24</b>
B.1	Basic Microlensing Parameters . . . . .	24
B.2	Finite Source Effects . . . . .	25
B.3	Microlens Parallax . . . . .	26
B.4	Astrometric Microlensing . . . . .	28
B.5	Measuring Lens Flux . . . . .	28
<b>C</b>	<b>Appendix: Finding Habitable Zone Planets with <i>WFIRST</i></b>	<b>30</b>
<b>D</b>	<b><i>Euclid</i> Microlensing</b>	<b>31</b>
D.1	<i>Euclid-WFIRST</i> Mass Measurements of Free-Floating Planets . . . . .	31
D.2	Early <i>Euclid</i> Imaging of the Bulge . . . . .	32

## 1. Introduction

The Wide-Field Infrared Survey Telescope (*WFIRST*) microlensing survey will be the most powerful microlensing survey ever undertaken, detecting an order of magnitude more microlensing events than available from the ground, and characterizing them with much higher precision. As a result, it will detect thousands of exoplanets ranging from a few lunar masses to super-Jupiters. More details about the *WFIRST* exoplanet survey can be found in the *WFIRST*-AFTA Science Definition Team Final Report (Spergel et al. 2013). Because *WFIRST* microlensing represents a major advance in microlensing capability, it will be able to reach new areas of the bulge and regularly observe microlensing effects rarely measurable in ground-based observations. As a result, unlike all previous microlensing surveys, *WFIRST* will be able to routinely measure the masses of many of its planets and their host stars.

The purpose of this SAG is to consider ways of reducing the technical risk of the *WFIRST* microlensing survey, as well as maximizing and expanding its science potential. We have identified several programs that are critical for enabling the following three key areas:

1. **Absolute planet mass measurements with *WFIRST*,**
2. ***WFIRST* field selection and simulations,**
3. **Development of microlensing expertise.**

These topics will be discussed in further detail below. Sections 2–8 will then discuss specific programs that can address these points. The first program, described in Section 2, is optical *Hubble Space Telescope* (*HST*) imaging of the entire *WFIRST* field that can be used to validate *WFIRST* astrometric microlensing measurements, which will be used to measure planet masses. These *HST* data can also be used to measure the source luminosity function in the bulge. The second program is a ground-based, near-IR microlensing survey (Section 3) that will provide concrete data on the expected near-IR microlensing event rates in the *WFIRST* field, reducing our reliance on extrapolation and Galactic models for predicting *WFIRST* yields and finalizing field selection. Sections 4–6 discuss observational programs to measure microlens parallax, lens fluxes, and astrometric microlensing of current microlensing events, supporting the continued development of techniques *WFIRST* will use to measure lens and planet masses. Sections 7 and 8 discuss programs that can help us meet the challenge of analyzing the *WFIRST* microlensing data. Our conclusions are given in Section 9. The appendices provide background information and explore topics outside of the scope of the main report.

### 1.1. *WFIRST* Planet Masses

**The most important need is to maximize the number of lens mass and thus planet mass measurements that can be made for *WFIRST* microlensing events.**

Aside from the sheer number of microlensing events, a key advantage of *WFIRST* over ground-based microlensing surveys is its ability to routinely measure lens masses (Appendix B). While *WFIRST* microlensing will robustly measure *mass ratios* ( $q = m_p/M_L$ ) for exoplanets, accurately determining the *masses* of those planets requires accurately measuring the masses of the lens (host) stars. Because of the higher resolution and better photometric accuracy available from space, *WFIRST* can take advantage of a variety of techniques for measuring or inferring the masses of the lenses that are rarely available from the ground (Bennett & Rhie 2002; Bennett et al. 2007). In many cases *WFIRST* will measure lens masses from measurements of the lens flux, microlens parallax (Gould 2013; Yee 2013), or measurements of astrometric microlensing (Gould & Yee 2014). However, while the theory of these various techniques for measuring masses is well understood, to date, they have only been practically applied in a handful of cases (e.g., Bennett et al. 2006; Gaudi et al. 2008; Janczak et al. 2010). It is vital that we continue to develop expertise in these areas in preparation for the *WFIRST* mission. We must also be able to vet these measurements to confirm their accuracy in the face of unknown systematics.

If the true planet masses are measured for a large fraction of *WFIRST* events, they can reveal detailed structure in the planetary mass distribution. In addition, because a measurement of the lens mass gives a measurement of its distance from the Earth, true planet masses also mean measurements of the planet frequency as a function of Galactic environment. Furthermore, these mass measurements can be used to identify microlensing events caused by old brown dwarfs, stellar-mass black holes, and neutron stars, objects that cannot otherwise be found unless they have luminous companions.

### 1.2. Field Selection

**The second need is to improve characterization of the *WFIRST* fields.**

A number of assumptions and extrapolations are used in the microlensing simulations for *WFIRST*. Currently, we rely either on theoretical models of the Galaxy, such as the Besançon model (Robin et al. 2003), or on the source luminosity function measured from Baade’s window combined with microlensing event rates extrapolated from optical microlensing fields. There are already suggestions of conflict between the measured optical, microlensing event rates and those predicted by Galactic models (Sumi et al. 2013), which implies more severe uncertainties going redward in wavelength into the near-IR and going spatially in toward the Galactic center.

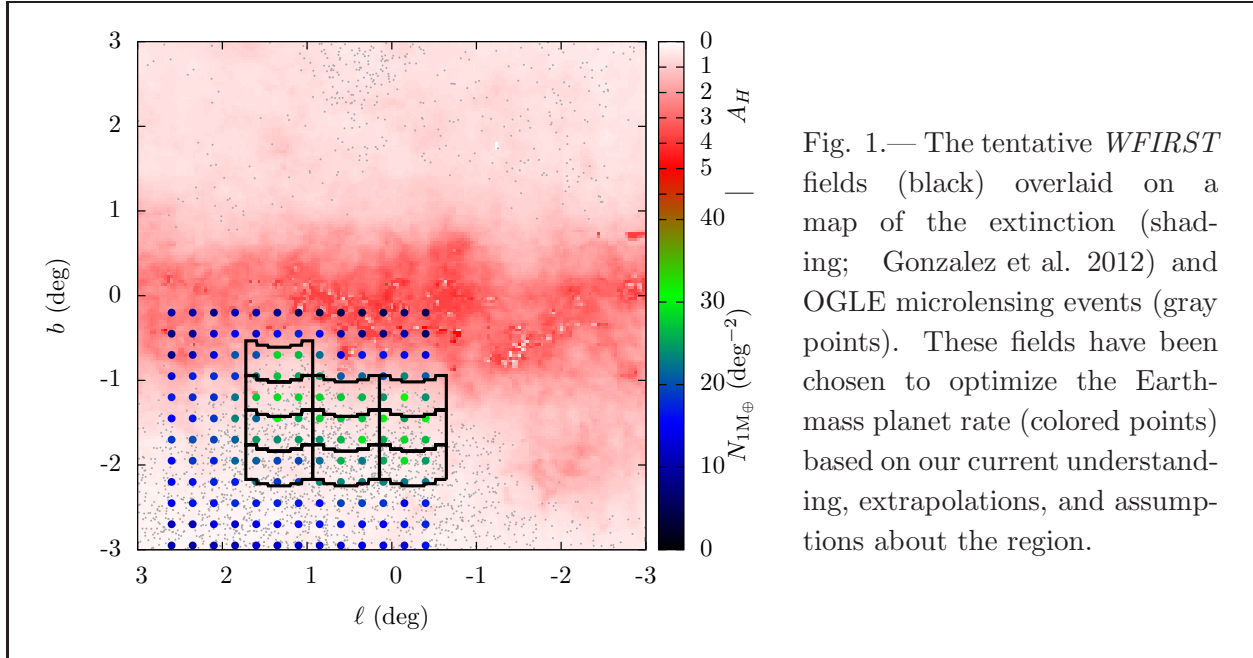


Fig. 1.— The tentative *WFIRST* fields (black) overlaid on a map of the extinction (shading; Gonzalez et al. 2012) and OGLE microlensing events (gray points). These fields have been chosen to optimize the Earth-mass planet rate (colored points) based on our current understanding, extrapolations, and assumptions about the region.

The *WFIRST*-AFTA report (Spergel et al. 2013) specifically cites the need to accurately measure

- the source luminosity function,
- the near-IR event rate,
- the relative bulge-to-disk planet frequency.

The exact placement of the *WFIRST* fields has not been finalized. Improving these assumptions or replacing them with data is necessary for accurately predicting the planetary yields and optimally selecting the *WFIRST* fields.

### 1.3. Microlensing Techniques

**The third need is continued development of microlensing techniques.**

The *WFIRST* microlensing mission will produce an enormous data set whose analysis will be a massive undertaking. Moreover, *WFIRST* will routinely measure higher-order light curve effects (Appendix B) that are rarely observed from the ground. In preparation for the launch of *WFIRST*, it is vital to develop human potential and experience with microlensing as well as the analysis tools that will be used for the *WFIRST* microlensing mission. As such, we place particular emphasis on programs that will develop the techniques important to *WFIRST*.



## 2. Optical *HST* Imaging of the *WFIRST* fields

Immediate optical *HST* imaging of the *WFIRST* fields will allow proper motion measurements for a substantial fraction of *WFIRST* stars, which provides a direct test of *WFIRST* astrometric microlensing measurements. These measurements are vital for measuring the masses of planets with faint or non-luminous hosts.

*WFIRST* has several techniques at its disposal for measuring lens masses (Appendix B), but the situation is fundamentally different for luminous and non-luminous lenses. For luminous lenses, direct detection of lens flux, combined with the image elongation and color-dependent centroid shifts that this induces over the course of the mission, yield lens mass measurements (Spergel et al. 2013). For non-luminous lenses, mass measurements require both measurements of  $\theta_E$  and  $\pi_E$  from higher-order microlensing effects. Astrometric microlensing is an important component of those measurements and essential for events with planets detected without caustic crossings (as well as isolated black holes and neutron stars). The optical *HST* observations proposed here are necessary to understand the systematics in the astrometric techniques so that we can extend *WFIRST*'s ability to measure masses to non-luminous lenses.

### 2.1. Astrometric Microlensing

Figure 2 illustrates the astrometric microlensing effect<sup>1</sup> that arises because the lensing of the source shifts the observed centroid of the light. By measuring these small centroid shifts, we can measure both the angular size of the Einstein ring,  $\theta_E$ , and the the lens-source relative proper motion,  $\mu_{\text{rel}}$ . These measurements can be combined with other information, one-dimensional parallaxes in particular, to yield mass measurements for the lens stars (see Appendix B for more details). Because astrometric microlensing only relies on detecting the light from the source, it provides a crucial tool for measuring masses of faint or dark lenses (e.g. brown dwarfs or black holes) and their planets. Furthermore, because astrometric microlensing also measures  $\theta_E$ , it supplies a critical piece of information necessary for measuring masses for isolated (point lens) objects and two-body events without caustic crossings (see Appendix B).

However, most astrometric microlensing measurements will be close to or at the limit of the noise (Gould & Yee 2014). The magnitude of the centroid shift due to astrometric microlensing,

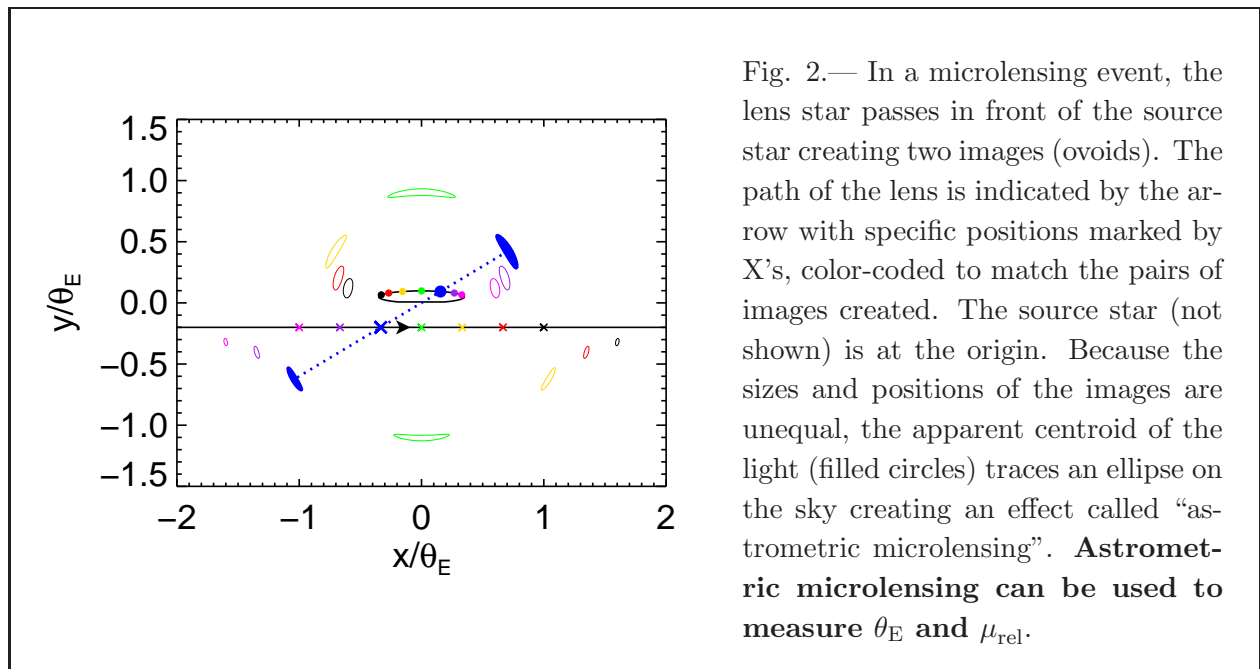
---

<sup>1</sup>“Astrometry,” the measurement of the precise location of a target, appears in several different contexts throughout this report. In this section, we discuss *astrometric microlensing*, which is the effect of the lensing on the measured astrometry. The *HST* observations proposed in this section are also astrometry, in that the key point is to measure the current positions of the future lenses and sources. In addition, the color-dependent centroid shifts described in Section 5 and Appendix B.5 are essentially astrometry. Finally, Section 2.4 uses astrometry in the traditional sense to compare *WFIRST* measurements of the positions of stars *en masse* to what is possible with *Gaia*.

$\Delta\theta_{\max}$ , is given by:

$$\Delta\theta_{\max} = \frac{\theta_E}{2\sqrt{u_0^2 + 2}} \sim 0.2 \text{ mas} \sqrt{\frac{M_L}{0.3M_\odot} \frac{\pi_{\text{rel}}}{0.125 \text{ mas}}}, \quad (1)$$

where  $M_L$  is the lens mass and  $u_0 \lesssim 1$ . To date, no measurements of this effect have been published because they require high precision astrometry, which will only be routinely available for microlensing events observed from space. Hence, it is vitally important to have robust proper motion measurements for a substantial number of *WFIRST* events to validate this technique. This is only possible by comparison to *HST* imaging of the *WFIRST* field made in the optical, 10 years in advance of the *WFIRST* microlensing mission.



## 2.2. Program Description

Optical, single-epoch, imaging with *HST* that covers the entire *WFIRST* field would vastly increase the value of the *WFIRST* microlensing survey. The primary goal of such imaging would be to separately resolve the future source and lens stars. The current lens-source separation, divided by the time baseline between the *HST* observations and the observed microlensing event, directly yields a measurement of their relative proper motion. This need to measure proper motions for a substantial fraction of *WFIRST* events drives the design of the program.

First, it is critical that the observations be undertaken immediately. In observations taken now (10 years before the *WFIRST* mission), 22% of sources and lenses are separated by at least 80 mas (i.e., are resolvable), but that number declines rapidly as we get closer to the *WFIRST*

launch date ( $N \propto \exp(-\Delta t)^2 \rightarrow 16\%$  and  $9\%$  with a time baseline of 9 and 8 years, respectively). Second, the observations must be done in the optical, where the diffraction limit is lower, in order to resolve as many source-lens pairs as possible. Finally, we note that previous observations of the bulge are insufficient to meet the goals of this program. To date, *HST* coverage of the inner bulge has been sparse. There are only 5 sets of *HST* fields within the proposed *WFIRST* survey area. These cover  $< 5\%$  of the *WFIRST* field and are heavily biased to the lower extinction, higher  $|b|$  part of the field. Hence, to measure proper motions of a significant fraction of *WFIRST* events requires new observations.

Because of the size of the *WFIRST* field, imaging the entire field in just one optical band will require  $\sim 750$  pointings of *HST*. While this number is large, the program could be split into several stages to be undertaken over multiple cycles. To begin with, sparse, preliminary observations in both F814W(*I*) and F555W(*V*) can be used to assess the necessary depth and extent of the imaging (especially the utility of F555W data in highly extinguished fields). These initial fields will focus on those guaranteed to be part of the final *WFIRST* field, since while the field may undergo some optimization, it will almost certainly have significant overlap with what is proposed now. These initial *HST* fields can be followed by a larger program to capture a larger area, and additional, targeted observations for regions where previous data show it is beneficial to go deeper. In addition, while optical data are being taken with ACS, complementary data in F160W(*H*) or F105W(*Y*) can be taken simultaneously (see Section 7).

### 2.3. Additional *WFIRST* Microlensing Science

Optical *HST* imaging has several benefits in addition to measuring relative proper motions for a large subset of *WFIRST* events. First, the improved accuracy of the positions and proper motions of the stars from the optical data will also improve the data reduction of the fields. Second, direct detections of the flux from the lens stars will be another means for *WFIRST* to estimate lens masses in cases where the lens is luminous. These optical data will provide additional colors that will improve characterization of these lenses. Also, the luminosity functions derived from these data will improve our understanding of the stellar populations in these fields, leading to better simulations of the *WFIRST* microlensing survey and improving estimates of the event rate and planet yields. Finally, *HST* relative proper motion measurements can give measurements of  $\theta_E$  (Equation B3) for events without finite source or astrometric microlensing measurements;  $\theta_E$  is a crucial parameter for microlensing planetary mass measurements.

Taken to the extreme, a 2-epoch, proper motion survey with *HST* could be used to search for stellar streams that provide more favorable conditions for detecting planets in the habitable zone (see Appendix C). The observed distribution of proper motions can also be used to improve Galactic models and therefore predictions for microlensing event rates.

## 2.4. Other Science

In addition to the direct benefits to the exoplanet mission, optical *HST* imaging can benefit the *WFIRST* mission in several other ways. Most strikingly, the *WFIRST* microlensing mission will provide a wealth of astrometric data on the Galactic bulge. *Gaia* will produce parallaxes for some of the stars in the bulge. However, the *WFIRST* relative parallaxes on these same stars will be  $\gtrsim 100$  times more precise. Furthermore, *WFIRST* will obtain relative parallaxes for millions of additional stars, below the *Gaia* magnitude limit, with a precision of  $\sigma(\pi) < 4 \mu\text{as}$  for 40 million stars and  $\sigma(\pi) < 10 \mu\text{as}$  for an additional 120 million stars. *WFIRST* relative astrometry can be transformed to the absolute *Gaia* astrometric system with a precision of  $\ll 1 \mu\text{as}$ . When the *WFIRST* data are combined with optical data, these additional colors can be used to disentangle temperature, extinction, and metallicity of stars and hence, measure detailed structure of the Galaxy including the structure of the Galactic bar and spiral arms, as well as obtain stellar age distributions along the line-of-sight from the Sun to the Galactic center. Finally, where the *HST* imaging overlaps with ground-based microlensing fields, the data can be used to measure lens fluxes (and hence, masses) for events discovered from the ground (see Section 5).

## 3. Ground-based, Near-IR, Microlensing Survey

**A ground-based, near-IR microlensing survey of the Galactic bulge would allow a direct measurement of the microlensing event rate in the *WFIRST* fields.**

### 3.1. Unknown Event Rate in the *WFIRST* Field

The *WFIRST* microlensing survey will be conducted in the near-IR. This allows *WFIRST* to probe deeper into regions of the Galactic bulge that have been inaccessible to optical surveys because of the high extinction. Our understanding of microlensing in these fields and in this band is limited to extrapolations from optical surveys in less extincted regions. Hence, simulations of the *WFIRST* microlensing survey are fundamentally limited by the lack of information about the fields.

Modeling of the inner Galaxy is an area of ongoing research. As such, there are still many uncertainties and some discrepancies. For example, there is significant dispersion among the predictions of the microlensing event rates from various models. Also, the recent measurement of the microlensing optical depth from the MOA survey, which only partially overlaps with the *WFIRST* field, is discrepant by as much as  $2.8\sigma$  from the predictions of Galactic models (Sumi et al. 2013). These problems could be even more severe for the parts of the *WFIRST* field that are not covered by optical data. For instance, Sumi et al. (2013) estimate the microlensing event rate is 30-60%

higher than the values used in the original Science Definition Team Final Report (Green et al. 2012). The only way to resolve these discrepancies is by obtaining more data. *In order to make good predictions for WFIRST microlensing, we need measurements of the microlensing event rate across the WFIRST field in the near-IR.* Ultimately, these measurements may affect the ultimate field placement.

### 3.2. Description of the Survey

We can measure the near-IR microlensing event rate from the ground for bright microlensing events by conducting a microlensing survey in the near-IR. This survey would cover all of the proposed *WFIRST* region, areas deeper into the bulge, and overlap with the highest cadence optical fields. It requires a good site in the southern hemisphere and an IR camera with a large field-of-view. The ideal survey would be dedicated to microlensing observations for the duration of the bulge season (April-September) and achieve a cadence of  $1 \text{ hr}^{-1}$ , which is necessary for a microlensing planet search. Based on these requirements, the best existing facility for such a survey is the VISTA telescope in Chile. Although the VVV program on the VISTA telescope will nominally carry out a microlensing survey, the observing cadence and duration is not actually optimized for microlensing observations or planet detection and do not meet the criteria specified above. Hence, a microlensing survey to measure the near-IR microlensing event rate would best be performed as a separate survey. Options beyond the VISTA telescope should be explored. For example, although its field-of-view is smaller and observing season shorter, a survey with UKIRT could achieve some of the major goals discussed here. Another alternative would be to build a wide-field IR camera and telescope such as the proposed WiFCOS camera coupled with the proposed Japanese telescope in Namibia.

### 3.3. *WFIRST* Science Outcomes

The primary purpose of the near-IR microlensing survey would be to directly measure the event rate as a function of Galactic coordinates. In regions of overlap with the optical, it will provide a direct comparison of the microlensing event rates in the optical and IR and quantify the relationship between them. This is important because optical microlensing can reach much fainter events from the ground as compared to observations in the IR.

In addition to event rates, the survey will provide measurements of the near-IR source fluxes for the microlensing events. These observations can be used to characterize the source population. Together with the event rates, and possibly luminosity functions from *HST* (Section 2), these measurements can be used to improve simulations of the *WFIRST* fields and probe the uncertainties in the Galactic models. All of this will help us to optimize *WFIRST* field selection.

Moreover, a near-IR microlensing survey can find giant planets in the inner bulge where the

extinction is too high for optical surveys. These are only the tip of the iceberg of what will be found by *WFIRST*. Incidentally, in the innermost regions of the bulge, the event timescale gives a strong indication of the distance of the lens from the Galactic center (Gould 1995). Hence, these planets can be used to estimate the relative frequency of planets in the bulge and the disk without direct knowledge of the lens mass. This is another unknown parameter that affects field selection and contributes uncertainty to *WFIRST* simulations.

Finally, we note that once such a survey is established, it could be continued into the *WFIRST* era to yield additional microlensing parallax measurements (see Appendix B.3). Because the baseline between a geosynchronous orbit and the Earth is quite short, satellite parallax effects (Section 4) will only be visible for the highest magnification events. Fortunately, this is the same subset that will be visible from the ground, where observations will be limited to the brightest (most highly magnified) targets because of the sky background. The situation is more favorable if *WFIRST* is at L2 because of the longer baseline (Yee 2013).

### 3.4. Other Science

The immediate science benefit for ground-based microlensing from a near-IR survey extends beyond the detection of additional planets in the expanded survey area. The overlap with ground-based, optical fields will give near-IR data on optical microlensing events, which can provide important, additional information. Measurements of the source fluxes in the near-IR improve the accuracy of lens flux measurements made with high-resolution imaging, which is primarily done in the near-IR (see Section 5 and Appendix B.5). These lens flux measurements lead to measurements of the masses and distances of the lenses. Additionally, IR data can be used to check for chromatic effects in the light curves such as lensing of starspots (Gould et al. 2013) or lensing of binary sources (Gaudi 1998; Hwang et al. 2013).

## 4. Satellite Parallaxes

**Satellite observations of ground-based microlensing events will vastly increase the number of mass measurements for microlensing planets. The resulting distance measurements can be used to probe the relative frequency of planets in the bulge and the disk, which could affect *WFIRST* field selection.**

### 4.1. Microlensing Satellite Parallax

In ground-based microlensing, it is difficult to determine the properties of the lens star, including its mass, unless microlens parallax is measured during the event. However, if this effect is

measured, it is possible to measure the mass of the lens star and its planet.

Microlens parallax effects arise because microlensing is a line-of-sight phenomenon. As such, observations of the same event from two different locations, such as the Earth and a satellite, can yield very different light curves due to parallax effects (Figure 3). The observable is  $\pi_E = \pi_{\text{rel}}/\theta_E$ , the trigonometric parallax scaled to the size of the Einstein ring. Appendix B shows that if both microlens parallax and  $\theta_E$  are measured, this gives a measurement of the lens mass (Equation B1).

Larger baselines lead to larger parallax effects, so satellites well-separated from the Earth are the ideal platforms for these observations. To date, only two such measurements have ever been made. The first used the *Spitzer* spacecraft to measure the parallax of a binary lens in a microlensing event toward the Small Magellanic Cloud (Dong et al. 2007). The second was a parallax measurement of a microlensing planet using the *Deep Impact* spacecraft (Muraki et al. 2011).

Over 100 microlens parallax measurements per season are possible if observations from a dedicated satellite at  $\sim 1$  AU are combined with ground-based observations. Both *Spitzer* and *Kepler* are well-suited for such dedicated campaigns to measure this effect. In addition, *TESS* may also be useful for serendipitous measurements of microlens parallax.

#### 4.2. *Spitzer* parallaxes

*Spitzer* can observe the Galactic bulge simultaneously with ground-based observatories for 40 days a year. Due to its narrow field-of-view, these observations would be targeted based on identification of microlensing events from ground-based survey data. Dedicating the satellite to microlensing observations during the 40 days (800 hours) will yield masses for 4–5 planets, including 1–2 planets discovered by the satellite, as well as microlens parallax measurements for about 120 events. In addition to the exoplanet science, this will identify brown-dwarf microlensing binaries and provide a more accurate estimate of the stellar mass function (Han & Gould 1996). A pilot program of 100 hours has been approved for Cycle-10. However, only the full, 800-hour program is capable of independently detecting planets.

#### 4.3. *Kepler* parallaxes

A *Kepler* microlensing mission complements a *Spitzer* microlensing mission. Because of its large field-of-view and predefined observing program, the mission would target a specific subfield within the larger *Kepler* field-of-view. This field would be selected to have the highest microlensing event rate as determined from ground-based surveys. As such, the *Kepler* mission will capture any microlensing events that occur in this field during the observational campaign, which can be identified afterwards from ground-based data, but it will miss events outside of its field. Hence, the

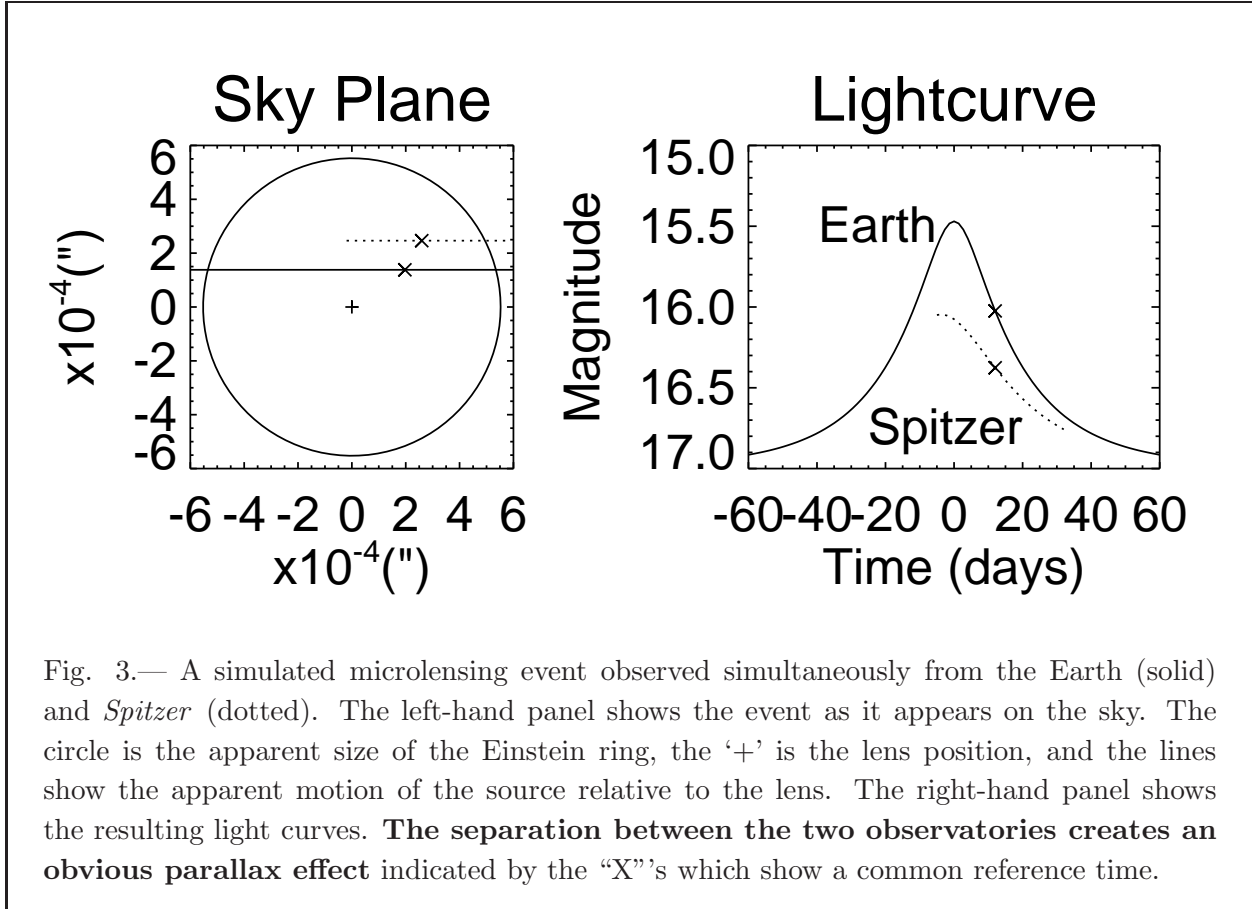


Fig. 3.— A simulated microlensing event observed simultaneously from the Earth (solid) and *Spitzer* (dotted). The left-hand panel shows the event as it appears on the sky. The circle is the apparent size of the Einstein ring, the ‘+’ is the lens position, and the lines show the apparent motion of the source relative to the lens. The right-hand panel shows the resulting light curves. **The separation between the two observatories creates an obvious parallax effect** indicated by the “X”’s which show a common reference time.

selection effects for a *Kepler* survey and a *Spitzer* survey will be substantially different, as will the actual events observed.

A *Kepler* microlensing mission would enable mass measurements for about 10 planets, half of which will be discovered by *Kepler*. In addition to achieving similar science goals to the *Spitzer* microlensing mission, because *Kepler* is not targeted and captures the whole field, it can improve our understanding of free-floating planet candidates. Currently, the detection of free-floating planets relies on statistical arguments that require a population of free-floating planets in addition to the stellar population in order to explain the excess of microlensing events with short timescales (Sumi et al. 2011). Through parallax measurements, *Kepler* can identify whether specific free-floating planet candidates are actually due to stellar lenses or rule out that possibility. Furthermore, *Kepler* is the perfect pilot for a dedicated microlensing parallax satellite designed for simultaneously observing all microlensing events for parallax (Gould & Horne 2013).

A microlensing mission is currently planned as part of *K2*. The NGC 2158 observations taken in Campaign 0 will serve as a test data set for developing a crowded-field *K2* reduction pipeline. Field 9 (to be observed in 2016) was specifically chosen to overlap with the ground-based microlensing



fields. Optimizing this field to cover the microlensing fields with the highest event rate can influence the expected yield by a factor of  $\sim 1.5$  compared to fields  $\sim 5$  degrees away. *A microlensing parallax survey with Field 9 offers the opportunity for unique science, especially since the proposed shutdown of Spitzer would prevent the realization of the parallax survey proposed in the previous section.*

#### 4.4. *TESS* parallaxes

As part of its planned transit observations, *TESS* will observe portions of the Galactic bulge that overlap the ground-based microlensing fields. Hence, it will observe any microlensing events that occur within its fields during normal observations, which could be analyzed for microlensing parallax signals. Because the *TESS* baseline is short ( $\lesssim 10^{-3}$  AU) and the satellite is designed to observe the brightest stars (albeit with much higher precision than necessary for microlensing), parallax measurements will only be possible for the highest magnification events or very bright events with caustic crossings (e.g. planetary signals) that occur while *TESS* is at apoapse. However, if any such events do occur, they will be identifiable from ground-based data, and all that will be required is to analyze the serendipitous *TESS* data.

If a bright, high-magnification event occurs during the *TESS* observations this offers the opportunity to measure not only Earth-*TESS* parallax but also a parallax signal from *TESS* itself as it executes its highly-elliptical orbit (Appendix B.3). This would be the first measurement of parallax from satellite orbital motion. If *WFIRST* is in geosynchronous orbit, such measurements will be the primary means to measure the second component of the microlens parallax vector for events with peak magnification  $\gtrsim 20$  (Gould 2013). This gives a complete parallax measurement, rather than a one-dimensional parallax, which is necessary to measure planet masses.

#### 4.5. Direct Relevance to *WFIRST*

Satellite parallax observations of ground-based microlensing events will yield planetary mass measurements as well as providing opportunities for additional planet detections. These observations will benefit *WFIRST* by contributing to our (currently nonexistent) understanding of the relative frequency of planets in the bulge and the disk. Furthermore, these will build expertise in parallax measurements, which will be ubiquitous in the *WFIRST* data, albeit in a somewhat different form (see Appendix B.3). They can also characterize the stellar mass function toward the bulge, which could influence *WFIRST* simulations and field selection.

In addition, if *Euclid* microlensing observations are ongoing at the time of the *WFIRST* microlensing survey, it is possible to measure satellite parallax effects between the two observatories. This offers an opportunity to directly measure masses for *WFIRST* free-floating planet candidates. Synergies between *Euclid* and *WFIRST* are discussed in detail in Appendix D.

Finally, *Kepler* observations could serve as a pathfinder for a small satellite mission to be flown simultaneously with *WFIRST* for the purpose of measuring robust parallaxes for the large majority of *WFIRST* events (Gould & Horne 2013). The requirements for such a mission are much less stringent than for the actual *WFIRST* mission since the events and their positions as well as the existence of planets can be identified from the *WFIRST* data. A dedicated parallax satellite can be positioned at  $\sim 1$  AU from *WFIRST*, a better separation for parallax measurements than the Earth-L2 baseline between *WFIRST* and *Euclid*. *Kepler* microlensing observations can help to specify the exact requirements of such a mission. For example, comparing the *Kepler* and *Spitzer* microlensing events will clarify the trade-offs entailed by larger pixels.

## 5. Lens Flux Measurements of Current Microlensing Events

**The mass of microlensing stars and planets can be directly measured if the light from the lens stars is measured with high-resolution imaging.**

### 5.1. Detecting Light from the Lenses

Microlensing can detect planets around distant, low-luminosity hosts. However, one of the main complications of ground-based microlensing observations is that the Galactic bulge microlensing fields have such a high stellar density that individual, main-sequence stars are not resolved. Thus, there will often be excess light in the seeing disk of the source in addition to the light from the source and the lens. This makes it difficult to isolate the light from the lens star and prevents the lens, and its planet, from being characterized.

The solution is to take high-resolution images sensitive enough to detect low-mass stars (Appendix B.5). These observations may be done while the lens and source are still superposed or after waiting several years for the lens and the source to separate. However, if the observations are taken while the lens and source are still superposed, in some cases there is a risk of ambiguous results. While the various probabilities can be calculated, there is a possibility that the excess flux is not due to the lens but due to a companion to the source or an extremely unlucky, chance superposition of an unrelated star (Janczak et al. 2010). This ambiguity can be resolved by measuring the relative proper motion between the excess flux and the source itself to ensure that the motion is consistent with the predictions from the microlensing light curve. With high-resolution images that reach the diffraction limit and are taken a number of years after the event, it is possible to resolve the lens and source stars, and therefore to verify the lens-source relative proper motion measured from the planetary microlensing light curve (Batista et al. 2014, in prep).

## 5.2. Current Capabilities

These observations may be taken from the ground using adaptive optics with an 8-meter class telescope or, even better, from space using *HST*. Because AO observations must be done in the near-IR, they require an estimate of the source flux in the near-IR. If near-IR observations were not taken during the microlensing event, this flux must be inferred from optical data. *HST* has the advantage that it can observe in the optical where the source flux is always known. In addition, because the diffraction limit is smaller, the source and the lens can be resolved much sooner using *HST*, enabling proper motion measurements. Alternatively, the association between the excess flux and the lens can be confirmed by measuring the color-dependent centroid shift from *HST* observations in multiple bands (Bennett et al. 2006).

Among other things, previous high-resolution observations have identified a massive, giant planet orbiting an M dwarf (Dong et al. 2009), a sub-Saturn mass planet likely to be in the Galactic bulge (Janczak et al. 2010), a cold super-Earth (Kubas et al. 2012), and a Jupiter in the habitable zone (Batista et al. 2014). Continued observations of this type will characterize more microlensing lens stars and lead to measurements of their planets’ masses. Furthermore, they will benefit *WFIRST* by building expertise in the technique and increasing our understanding of planet occurrence as a function of Galactic environment (Section 1.2).

## 6. Astrometric Microlensing Due to Black Holes

**Astrometric microlensing can be observed for microlensing events caused by black holes. Such observations will help develop the technique in advance of the *WFIRST* mission.**

Equation 1 shows that astrometric microlensing measurements are not usually possible without *WFIRST* precision ( $28 \mu\text{as}/\text{observation}$ ; Gould & Yee 2014). However, because the magnitude of the effect is proportional to the square-root of the lens mass, for the subset of events caused by stellar-mass black holes ( $\sim 10M_{\odot}$ ) the signal increases to  $\sim 1.1 \text{ mas}$ . In addition, candidate events can be easily identified because the size of the Einstein ring increases with increasing lens mass (Equation B1), and consequently, more massive objects have proportionally longer timescales (Equation B3), typically hundreds of days for black holes. Continued efforts to measure this effect using *HST* (e.g., Sahu et al. 2012) and adaptive optics will further the development of this technique, which will be vital to the *WFIRST* mission.

## 7. Multi-Epoch, Near-IR, *HST* Observations

**Multi-epoch, *HST*/WFC3/IR observations of a few fields in the bulge are necessary for developing the *WFIRST* pipeline and understanding how well a random dither pattern will characterize the *WFIRST* detector.**

Developing a robust photometry/astrometry pipeline for *WFIRST* is mission-critical. This process would benefit from test data with similar properties and systematics to the future *WFIRST* data. Such data do not currently exist.

One major concern is that overlapping stars in the crowded fields could induce systematics in the photometry and astrometry as the amount of the overlap changes as a function of time due to proper motion. A second concern is in understanding how well a random dither pattern samples the *WFIRST* detector. If the detector is properly sampled, *the WFIRST microlensing data will provide a multitude of point sources that can be used to understand the detector at a sub-pixel scale. Understanding the detector at this level is critical to the weak-lensing survey.* The same data needed to test the photometry/astrometry pipeline can also be used to test the usefulness of a random dither pattern in characterizing the *WFIRST* detector.

Multi-epoch observations of the bulge with *HST*/WFC3/IR would provide the data to achieve both of these goals. Such a program would require  $\sim 10$  orbits per season for a minimum of 3 seasons. This would give a time baseline of at least 2 years, enough to measure both parallax and proper motions for a select number of fields and to test the *WFIRST* pipeline. Simultaneous optical data will provide the higher resolution necessary to determine how well the pipeline can reconstruct the underlying star pattern. In addition, the IR data can be used to understand how well a random dither pattern will characterize the detector using crowded-field observations. Such a program could overlap with the *HST* observations described in Section 2 or Section 5.

## 8. Microlensing Analysis Challenge

**An open competition in microlensing analysis will encourage the development of novel techniques and attract new people to the field.**

### 8.1. Complexities in Microlensing Analysis

Many planetary microlensing events should be simple to model. Gould & Loeb (1992) and Gaudi & Gould (1997) show that the mass ratio and projected separation,  $q$  and  $s$ , can be easily estimated for a large subset of planetary, microlensing light curves. However, this will not be universally true, especially since *WFIRST*'s unprecedented photometric accuracy and homogeneous

data set will allow detailed investigation and modeling of higher-order lensing effects such as parallax and orbital motion. Furthermore, not all events will obey these simple relations. Of particular interest are planets in binary star systems, (i.e., triple lenses as in Gould et al. 2014), planets detectable without direct caustic crossings (e.g., Zhu et al. 2014), and planets in high-magnification microlensing events (Griest & Safizadeh 1998).

Although our techniques for solving microlensing light curves have grown quite sophisticated (e.g., Gould & Gauchere 1997; Dong et al. 2006; Cassan 2008; Bennett 2010; Bozza 2010), there still remain unsolvable light curves.

## 8.2. Parameters of the Challenge

One way to address this problem would be to hold an open competition in microlensing light curve analysis. This competition would be open to anyone, and in particular should seek out the participation of mathematicians and computer scientists. Bringing an outside perspective to the problem and drawing on a breadth of expertise can lead to the development of new algorithms and approaches to solving the multivariate and multi-modal microlensing likelihood space. Similar competitions have been carried out for weak lensing<sup>2</sup> and strong lensing<sup>3</sup>.

The basic elements of the competition would be to:

1. Provide a basic introduction to microlensing (e.g., Gaudi 2012),
2. Provide a set of microlensing light curves (real or simulated or both),
3. Establish a metric with which to evaluate the results.

The goals of the competition would be to

- Develop new analysis techniques,
- Develop robust and publicly available codes,
- Discover previously unknown degeneracies.

As an example, one could use the data from the microlensing survey proposed in Section 3 and inject planets into the light curves. This would lead to the recovery of the true planetary signals, and also a characterization of the overall sensitivity of the survey.

---

<sup>2</sup>great3challenge.info

<sup>3</sup>timedelaychallenge.org

There are significant logistical challenges to running such a competition. However, if it can be undertaken for a modest cost in time, money, and personnel, the potential benefits to *WFIRST* and the field could be substantial.

## 9. Conclusions

The programs explored by this SAG fall into the following major categories:

1. Programs that directly support *WFIRST* science and reduce its scientific risk:
  - Early, optical, *HST* imaging of the *WFIRST* field
  - A preparatory, ground-based, microlensing survey in the near-IR
2. Programs that develop experience with techniques for measuring planet masses:
  - Satellite parallax observations using *Spitzer*, *Kepler*, and *TESS*
  - *HST* or AO flux measurements of lenses in ground-based microlensing events
  - Measurements of astrometric microlensing for black holes
3. Programs that support the development of *WFIRST* analysis pipelines:
  - Multi-epoch *HST*/WFC3/IR observations of the bulge
  - An open competition in microlensing analysis

In our study of programs that will support and enhance the *WFIRST* microlensing mission, the program that is the most time critical and with direct relevance to the *WFIRST* mission is **optical *HST* precursor imaging of the proposed *WFIRST* fields**. The long time baseline between now and the *WFIRST* mission is crucial for measuring proper motions and separately resolving the source and lens stars, which will necessarily be superposed during the *WFIRST* microlensing events. Measured relative proper motions using *HST* are the best way to validate the astrometric microlensing measurements, which will be made by *WFIRST* and used to measure star and planet masses for faint lenses. Furthermore, these observations will not only inform *WFIRST* field selection by measuring the luminosity function in the *WFIRST* fields to faint magnitudes, but will also provide valuable data for characterizing the source and lens stars by providing additional colors that can be used as metallicity, effective temperature, and age diagnostics. These data will vastly enhance the *WFIRST* microlensing survey by enabling detailed studies of Galactic structure using precision astrometry from *WFIRST*.

The second program with direct relevance to the *WFIRST* microlensing mission is a **ground-based near-IR microlensing survey**. Such a survey would allow direct measurements of the near-IR microlensing event rates and source luminosity function in the *WFIRST* fields. Addi-

tionally, the near-IR data from this survey will provide concurrent observations of microlensing events where the field overlaps with the optical ground-based surveys. These data are important for adaptive optics or space-based luminosity measurements for the lens stars in those events.

In addition to these programs that directly support the *WFIRST* microlensing mission, we have identified a series of programs that will develop expertise and experience in the techniques that *WFIRST* will use to measure lens masses and locations. **Microlensing parallax observations by *Spitzer* and *Kepler*** would be the first systematic observations for microlens parallax using a satellite and would serve as pathfinders for a potential, small, dedicated microlensing parallax satellite. Likewise, ***HST* or adaptive optics observations of known microlensing planets** will measure masses for the host stars and planets by directly measuring the lens light, a technique that should be routine with *WFIRST* but requires additional observations and effort for ground-based microlensing. Because all of these programs will measure masses for microlensing planets, they will also measure their distances, and hence, will provide the first insight into the Galactic distribution of planets, which may allow optimization of the *WFIRST* fields for maximum planet detection. Similarly, **searches for astrometric microlensing signals from black holes** will promote development of a technique that will be frequently used by *WFIRST* but is rarely observed today.

Finally, we have identified several other programs of interest to *WFIRST*. **Multi-epoch *HST* observations** can be used to develop and test the mission-critical, *WFIRST* photometry/astrometry pipeline. **A microlensing analysis challenge** will develop expertise in and novel approaches to analyzing *WFIRST* light curves. Once *WFIRST* has been selected, we support the enactment of a special NASA program to fund *WFIRST*-related science, including the programs mentioned here.

### A. Appendix: Charter

Although the launch of the *WFIRST* mission is still many years off, it is nevertheless vitally important to consider what activities must be carried out in the near future in order to retire any scientific risks associated with, and maximize the returns from, the *WFIRST* microlensing survey. In particular, there may be projects that require a long time baseline and/or might affect the final mission design, and thus must be undertaken soon. This SAG will bring together members of the microlensing community to identify scientific programs that will benefit the *WFIRST* microlensing mission. Of particular interest are mission-critical observational programs that must be completed before the launch of *WFIRST*. Specifically, the major question this SAG will address is:

“What scientific programs can be undertaken now to ensure the success of the *WFIRST* mission and maximize its scientific return?”

In the process of answering this question, the SAG will:

1. Identify both mission critical and mission enhancing programs,
2. Identify immediate science to come out of each program, as well as the program’s direct impact on the *WFIRST* mission,
3. For each proposed program, quantify the improved scientific return for the *WFIRST* mission,
4. Emphasize programs that can be executed using existing (NASA) resources.



## B. Appendix: Introduction to *WFIRST* Microlensing

### B.1. Basic Microlensing Parameters

**The most important scale in microlensing is the size of the Einstein ring,  $\theta_E$ :**

$$\theta_E = \sqrt{\kappa M_L \pi_{\text{rel}}} \quad \text{where} \quad \pi_{\text{rel}} = \frac{\text{AU}}{D_L} - \frac{\text{AU}}{D_S} \quad \text{and} \quad \kappa = 8.14 \text{ mas } M_\odot^{-1}. \quad (\text{B1})$$

$M_L$ ,  $D_L$ , and  $D_S$  are defined as in Figure 4.

Planets are detected in microlensing light curves when one of the images of the source passes over or near the position of the planet<sup>4</sup>. Since the position of those images is determined by  $\theta_E$ , the inferred parameters of the planet are necessarily also measured relative to  $\theta_E$ . Specifically, the observables are  $q = m_p/M_L$ , the mass of the planet relative to the mass of the lens star<sup>5</sup>, and  $s = r_{\text{proj}}/(\theta_E D_L)$ , the position of the planet projected onto the lens plane relative to the size of the Einstein ring. Recovering the underlying properties of the planet requires the measurement of additional parameters.

The direct observable from the light curve is the source magnification as a function of time,  $A(t)$ . This magnification is set by the position of the source relative to the lens,  $u$ , measured as a fraction of the Einstein radius, i.e.,  $A(t) \rightarrow A(u)$ . Since the motion of the source in the lens plane is determined by the lens-source relative proper motion,  $\mu_{\text{rel}}$ , the value of  $u$  depends on this and the size of the Einstein ring, i.e.:

**All of the methods presented here for measuring  $M_L$  require that  $\theta_E$  also be measured. Hence, whenever  $M_L$  is measured, so is  $D_L$  (Equation B1).**

$$u = \sqrt{u_0^2 + \tau^2} \quad \text{where} \quad \tau = \frac{t - t_0}{t_E}, \quad (\text{B2})$$

$u_0$  is the impact parameter between the source and the lens,  $u = u_0$  at  $t = t_0$ , and

$$t_E = \frac{\theta_E}{\mu_{\text{rel}}}. \quad (\text{B3})$$

Although the basic microlensing light curve yields three observable parameters:  $t_0$ ,  $u_0$ , and  $t_E$ , only  $t_E$  encodes information about the underlying properties of the lens. Hence, we have only one equation (Equation B3) and three unknowns<sup>6</sup>:  $M_L$ ,  $D_L$ , and  $\mu_{\text{rel}}$ . Generally speaking, this is of limited utility.

<sup>4</sup>A more comprehensive review of microlensing can be found in Gaudi (2012).

<sup>5</sup>i.e., the size of the planet’s Einstein ring relative to the size of the star’s Einstein ring.

<sup>6</sup>The source can generally be assumed to be in the bulge, so  $D_S$  is generally well determined.

In the following sections, we discuss ways to break this degeneracy using additional observables so that we can measure  $M_L$  and  $D_L$  and recover the intrinsic properties of the planets  $m_p$  and  $r_{\text{proj}}$ . Each of these effects is optimized in a different parameter regime and has different systematics. Hence, measuring multiple effects for the same events provides an important comparison sample for quantifying these biases.

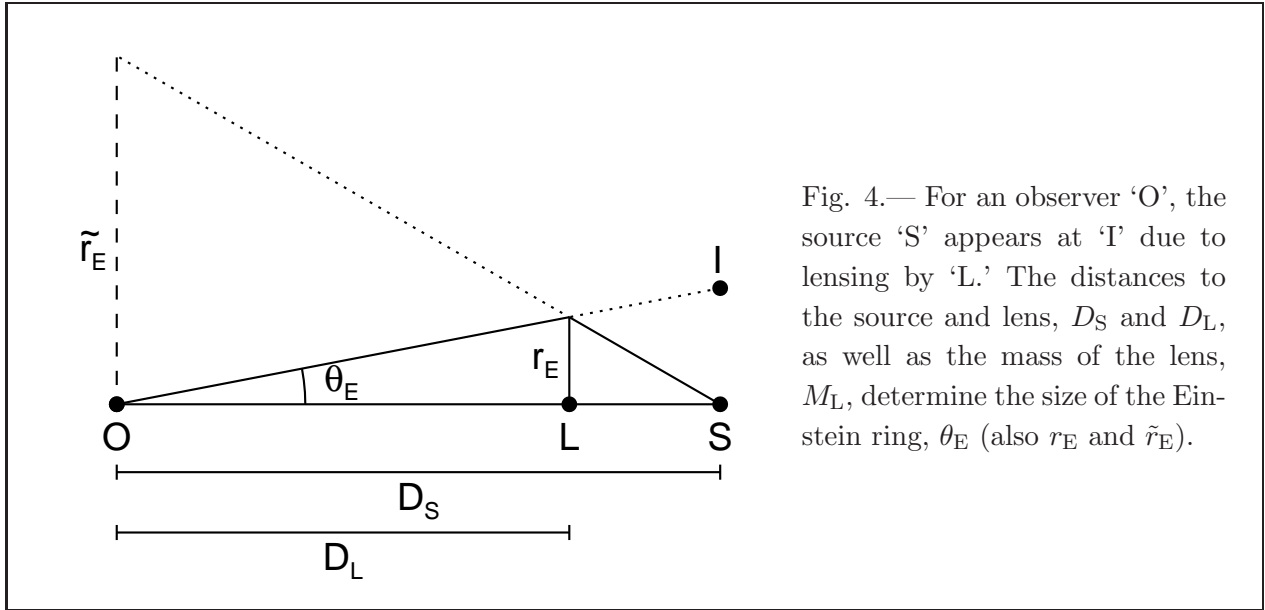


Fig. 4.— For an observer ‘O’, the source ‘S’ appears at ‘I’ due to lensing by ‘L.’ The distances to the source and lens,  $D_S$  and  $D_L$ , as well as the mass of the lens,  $M_L$ , determine the size of the Einstein ring,  $\theta_E$  (also  $r_E$  and  $\tilde{r}_E$ ).

### B.2. Finite Source Effects

$\theta_E$  can be measured if the size of the source is resolved by a caustic.

As a consequence of the equations of microlensing, certain values of  $u$  correspond to  $A(u) = \infty$  for a theoretically perfect, point source; these locations are called the “caustics”. For a point lens, the caustic is a single point at the position of the lens star. For a lens with a companion, the caustic is a closed curve with zero thickness but enclosing a finite area. If the source star passes over or very close to a caustic (a common occurrence if a planetary companion is detected), the fact that the source is not a perfect point source becomes relevant. The observed magnification is the integration of the magnification pattern across the face of the source star. Hence, in practice the magnification is never infinite and it takes a finite amount of time for source to cross the caustic, creating a rounded peak in the light curve (e.g. Gould et al. 2009). By measuring the width of this peak,  $2t_\star \sim 2\theta_\star/\mu_{\text{rel}}$ , we can determine the size of the source relative to the size of the Einstein ring,

$$\rho = t_\star/t_E = \theta_\star/\theta_E, \tag{B4}$$

where  $\theta_\star$  is the angular size of the source,  $R_\star/D_S$ .

The position of the source on the color-magnitude diagram can be combined with surface brightness relations (e.g. Kervella et al. 2004) to estimate  $\theta_*$  (Yoo et al. 2004). Thus, observing the effects of the finite size of the source in the light curve yields a measurement of  $\theta_E$  and consequently,  $\mu_{\text{rel}}$  (Equation B3). **Measuring  $\theta_E$  therefore provides a mass-distance relationship for the lens,** but does not completely resolve the degeneracy.

### B.3. Microlens Parallax

Changing or multiple lines of sight lead to parallax effects in the light curve.

Because the microlensing effect depends precisely on the *apparent* alignment of the source and lens stars, slight differences in the line-of-sight can affect the observed light curve. This parallax effect can be seen in two different types of circumstances. First, if there are observations from two different locations, the two observatories will see two different light curves, e.g. the “satellite” parallax effect between the Earth and a satellite (see Section 4, Figure 3). Second, orbital parallax effects can arise due to the acceleration of the observatory during the microlensing event as the observatory progresses through its orbit (Figure 5).

Parallax only affects the light curve by the amount it deflects the position of the lens relative to the size of the Einstein ring. Therefore, the observable microlensing parameter is the microlens parallax,  $\pi_E$ , which is related to the trigonometric parallax by

$$\pi_E = \frac{\pi_{\text{rel}}}{\theta_E}. \quad (\text{B5})$$

Hence, if *both*  $\pi_E$  and  $\theta_E$  are measured, they can be input into Equation B1 and both  $M_L$  and  $D_L$  are measured.

The major complication with microlens parallax is that it is a vector. The relative motion between the source and the lens is created by the combination of proper motion and parallax. The *magnitude* of the relative proper motion is the direct microlensing observable. Its direction is only relevant if parallax effects are also observed. Since the known direction of the observatory’s orbital motion or physical baseline sets the orientation of the parallax effect, this specifies the orientation of the microlensing event on the sky, and the direction of the proper motion. Hence, in microlensing, we typically consider the relative proper motion to be a scalar and the parallax to be a vector whose direction is the direction of the relative proper motion.

The biggest difficulty with measuring parallax, particularly orbital parallax, is that **one component of the parallax vector is much better constrained than the other.** Consider the fact that a typical microlensing event lasts much less than a year, during which Earth’s (or *WFIRST*’s) acceleration is effectively constant. The component of the parallax parallel to this direction is readily measured because it accelerates the timing of the light curve producing an asymmetry. In contrast, the perpendicular component of the parallax produces a symmetric dis-

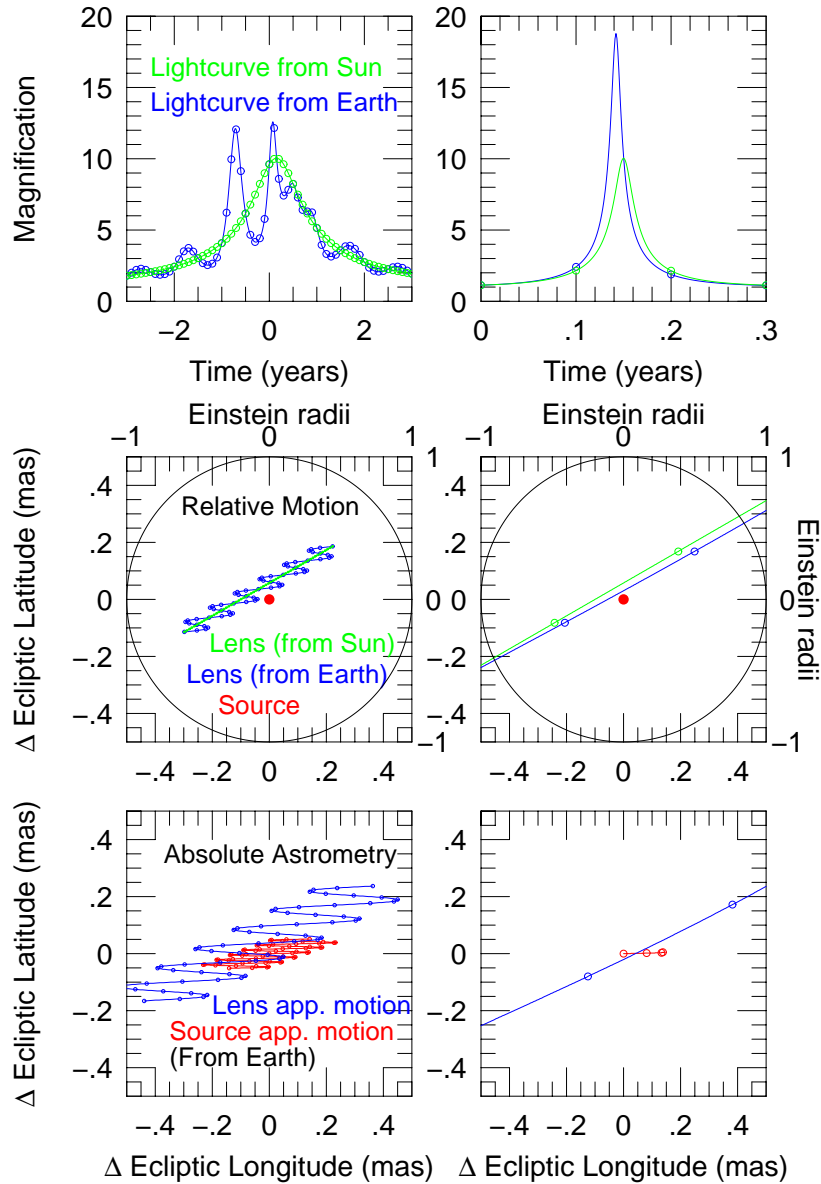


Fig. 5.— Figure 1 from Gould & Horne (2013). The orbital parallax effect for illustrative (left) and realistic (right) microlensing events. Microlensing events appear different from the Earth and the Sun because the Earth is an accelerating platform. Bottom: absolute trigonometric parallax and proper motion (ppm). Middle: relative trigonometric (lower/left labels) and microlensing (upper/right labels) ppm. Top: resulting light curves as seen from the Earth (blue) and the Sun (green). The same effect will be measurable from *WFIRST* as it orbits the Sun.

tortion which can be partially compensated for by other symmetric parameters of the light curve, e.g.  $u_0$  and  $t_E$ . Therefore, the parallel component is much more easily measured than the perpendicular component, so the parallax information can be incomplete. In fact, *WFIRST* is expected to measure a large number of one-dimensional parallaxes for its events, which will provide a statistical understanding of the underlying lens population (Han & Gould 1995), but will not give complete parallax measurements without additional information about the direction of the relative proper motion. This problem is particularly pronounced for objects in the Galactic bulge where the measurement uncertainties will be similar to the magnitude of the effect (Gould 2013).

#### B.4. Astrometric Microlensing

**The unequal size of the lensed images leads to a net shift in the centroid of the light that changes over the course of the microlensing event.**

Figure 2 illustrates the effect of astrometric microlensing (Walker 1995). For a point lens, the centroid of the source light appears to execute an ellipse. The expected position of the centroid relative to the size of the Einstein ring can be calculated exactly from the microlensing parameters  $t_0$ ,  $u_0$ , and  $t_E$ . Hence, the displacement of the observed centroid directly gives  $\theta_E$  and  $\mu_{\text{rel}}$ . In addition, **the direction of the motion of the centroid gives the *direction* of the lens-source relative proper motion, which is crucial for converting one-dimensional parallax measurements into complete measurements of  $\pi_E$ .**

This method provides an important complement to measuring  $\theta_E$  using finite source effects, which requires a caustic interaction. Such interactions are rare for point lens events; with mass measurements, these planet-less objects can provide an important comparison sample for the planetary microlensing hosts with measured masses. In addition, because of its precision photometry, *WFIRST* has the potential to measure more subtle planetary signals that do not require caustic crossings (Zhu et al. 2014). For these events, astrometric microlensing can be used to measure  $\theta_E$ .

#### B.5. Measuring Lens Flux

**Combining the mass-distance relation from Equation B1 with a luminosity-distance relation for the lens allows the lens mass to be determined.**

If the lens star is luminous, it is possible to detect its light in the presence of the source star. This may be done either when the lens is superposed or once it has separated slightly from the source. The main complication with doing this for ground-based microlensing events is that the seeing-limited PSF may contain light from several unrelated stars due to the density of stars in the Bulge. However, with *WFIRST*'s sensitivity and resolution, which can detect and resolve main

sequence stars in or near the bulge, the lens light can be measured directly. A measurement of the apparent magnitude of the lens combined with an extinction relation gives a relationship between the absolute magnitude of the lens and its distance. The mass-distance relationship given by  $\theta_E$  can be transformed into a second luminosity-distance relationship using stellar isochrones. Since these have different functional forms, their intersection determines the mass and distance to the lens.

The major complication of this method is the possibility of light contamination. Usually, the most likely origin for the excess light is the lens star, but the light could also come from a luminous companion to the lens or the source or, much less likely, an unrelated star that is still within the confusion limit for diffraction-limited images. The probabilities for all these scenarios can be quantified using non-detections from the microlensing light curve, knowledge about binary star fractions, and the average stellar density in the field. In addition, if some time has passed since the microlensing event, it is possible to measure the lens-source relative proper motion even if the two stars have not completely separated so as to be clearly resolved. This measurement can be checked against the value of  $\mu_{\text{rel}}$  from the light curve to confirm that the observed light is associated with the lens.

There are two methods that can be used for measuring the relative proper motion between the source and the putative lens star before they are clearly resolved. The first is the color-dependent centroid shift. If the lens is of comparable brightness to the source but has a different color, the centroid of the combined lens+source will be different when observed with different filters. *HST* follow-up images of the first two planetary microlensing systems have used this method to identify the lens stars for these events (Bennett et al. 2006; Dong et al. 2009). The second method is the elongation of the combined lens+source image as discussed by Bennett et al. (2007). Both of these methods require a stable point-spread-function (PSF) that can be obtained from a space telescope such as *WFIRST*. However, these two methods have only been applied in the few cases referenced here. As in the case of astrometric microlensing, the best way to validate these measurements and check for systematics is by comparison to proper motions measured from precursor *HST* imaging (Section 2).

*WFIRST* is expected to directly detect the lens star and its relative proper motion with respect to the source for more than 75% of planetary microlensing events in which the planetary host star is on the main sequence.

### C. Appendix: Finding Habitable Zone Planets with *WFIRST*

There is a possibility of increasing the number of habitable zone planets detected by *WFIRST* by biasing the survey toward fields with small  $r_E$ . However, the trade off is likely a substantial drop in the total number of planets detected.

The nominal *WFIRST* microlensing survey is expected to find a small number of  $\sim$ Earth-mass planets in the habitable zones of F-, G- and K-dwarfs, and a significant number of similar planets just outside their habitable zones (Penny et al. 2014, in prep).

The semimajor axis range that is probed for planets in a given microlensing event is set by the Einstein radius of the lens (Appendix B.1). The smaller the Einstein ring, the smaller the semimajor axis probed. Most habitable planets will lie inside the Einstein ring, where the detection efficiency scales approximately as  $(a/r_E)^3$ . In addition to lens mass, the physical Einstein ring radius depends on the distances to both the lens and the source

$$r_E = D_L \theta_E = D_L \sqrt{\kappa M_L \pi_{\text{rel}}}. \quad (\text{C1})$$

Therefore, for a lens of fixed mass, the physical Einstein radius will be smaller if the lens is either close to the source or close to the observer.

It is likely possible to find fields with an Einstein radius distribution skewed towards lower values relative to the fields optimized for the overall planet detection. For example, sight lines that exhibit counter moving stellar streams, such as those due to X-shaped structures in the bulge, (Poleski et al. 2013), may provide the necessary conditions for this. However, **our knowledge of both the kinematic and line-of-sight structure of the inner bulge is insufficient to predict the locations of such fields at present.** A two-epoch, two-color survey of the inner bulge with *HST* would measure the proper motion and line-of-sight distributions of the F, G, and K dwarf star populations, including the best candidates to be the hosts of habitable planets that are detectable by microlensing. This would allow the Einstein radius distribution for these stars, weighted by the microlensing event rate, to be robustly estimated and normalized, allowing a precise estimate and optimization of the effective number of habitable zones that would be probed by the *WFIRST* microlensing survey.

*If such a path were pursued, the boost in habitable planet detection efficiency gained by smaller Einstein radii would have to more than balance the drop in event rate sustained by moving to non-optimal fields.*

## D. *Euclid* Microlensing

**A *Euclid* microlensing mission concurrent with *WFIRST* is capable of measuring masses for individual free-floating planets.**

*Euclid* is expected to launch in 2020, in advance of the *WFIRST* mission. NASA is participating in this mission by contributing the near-IR imagers and a delegation of scientists. This spacecraft with its near-IR imager is well-suited to microlensing observations and imaging of the bulge (Penny et al. 2013). The scheduling of any microlensing observations will be likely be decided in 2015-2016. If a *Euclid* microlensing survey occurs, it would likely take place around 2024-2025, which is close to the time of the first *WFIRST* microlensing observations.

### D.1. *Euclid-WFIRST* Mass Measurements of Free-Floating Planets

If *Euclid* microlensing observations are simultaneous or ongoing with the *WFIRST* microlensing mission, this provides an opportunity to measure microlens parallax effects between the two satellites, and hence, more masses for lens stars and their planets. In fact, this provides the best opportunity for measuring the masses of free-floating planets. **Simultaneous observations from *Euclid* at L2 and *WFIRST* in geosynchronous orbit would be able to directly measure masses for 15% of  $10M_{\oplus}$  free-floating planets**, with the percentage of mass measurements increasing for smaller free-floating planets.

These microlensing observations could be enhanced by adding a third ground station for downloading *Euclid* data. With only two ground stations, the limits on the data rate mean that high-resolution optical data cannot be downloaded from *Euclid* with the same cadence as the near-IR microlensing data. *If NASA or ESA were to contribute a third ground station, Euclid would be able to use both its optical and near-IR imagers for a microlensing survey*, adding additional color information for its microlensing events. Among other things, such information can be used to confirm that the candidate free-floating planet events are indeed caused by microlensing (an achromatic effect) rather than some unknown astrophysical phenomenon, which would likely have some color dependence (e.g. Gould et al. 2013). Multi-band data can also be used to vet anomalous microlensing events whose light curves may be explained by either a 2-body lens or a binary source. If the proposed binary source has unequal mass components, the changing, differential magnification of the two sources will result in chromatic effects in the light curve (Gaudi 1998; Hwang et al. 2013).



## D.2. Early *Euclid* Imaging of the Bulge

During its commissioning, *Euclid* could conduct early imaging of the Galactic bulge. Deep, multiband (optical, *Y*, *J*, and *H*) observations could serve as a precursor to the *Euclid* microlensing mission. The optical data will be useful for characterizing the stars in the *WFIRST* field. The improved resolution over the near-IR will aid in proper motion studies of *WFIRST* stars and could improve *WFIRST* photometry because the positions of the stars will be better known. In addition, the optical luminosity functions will complement the data from *WFIRST*. However, these data will not replace precursor *HST* imaging (Section 2), because they will not have the time baseline or resolution to resolve the future sources and lenses, a requirement for measuring the relative lens-source proper motions. Hence, although an early epoch of multi-band data from *Euclid* may not be of substantial benefit to the *WFIRST* microlensing survey, it will certainly be beneficial for *WFIRST* science in general.

## REFERENCES

- Batista, V., Beaulieu, J.-P., Gould, A., et al. 2014, *ApJ*, 780, 54
- Batista, V., et al. 2014, in prep
- Bennett, D. P. 2010, *ApJ*, 716, 1408
- Bennett, D. P., Anderson, J., Bond, I. A., Udalski, A., & Gould, A. 2006, *ApJ*, 647, L171
- Bennett, D. P., Anderson, J., & Gaudi, B. S. 2007, *ApJ*, 660, 781
- Bennett, D. P., & Rhie, S. H. 2002, *ApJ*, 574, 985
- Bozza, V. 2010, *MNRAS*, 408, 2188
- Cassan, A. 2008, *A&A*, 491, 587
- Dong, S., DePoy, D. L., Gaudi, B. S., et al. 2006, *ApJ*, 642, 842
- Dong, S., Udalski, A., Gould, A., et al. 2007, *ApJ*, 664, 862
- Dong, S., Gould, A., Udalski, A., et al. 2009, *ApJ*, 695, 970
- Gaudi, B. S. 1998, *ApJ*, 506, 533
- . 2012, *ARA&A*, 50, 411
- Gaudi, B. S., & Gould, A. 1997, *ApJ*, 486, 85
- Gaudi, B. S., Bennett, D. P., Udalski, A., et al. 2008, *Science*, 319, 927
- Gonzalez, O. A., Rejkuba, M., Zoccali, M., et al. 2012, *A&A*, 543, A13
- Gould, A. 1995, *ApJ*, 446, L71
- . 2013, *ApJ*, 763, L35
- Gould, A., et al. 2014, *Science*, submitted
- Gould, A., & Gaucherel, C. 1997, *ApJ*, 477, 580
- Gould, A., & Horne, K. 2013, *ApJ*, 779, L28
- Gould, A., & Loeb, A. 1992, *ApJ*, 396, 104
- Gould, A., Udalski, A., Monard, B., et al. 2009, *ApJ*, 698, L147
- Gould, A., Yee, J. C., Bond, I. A., et al. 2013, *ApJ*, 763, 141
- Gould, A., & Yee, J. C. 2014, *ApJ*, 784, 64

- Green, J., Schechter, P., Baltay, C., et al. 2012, ArXiv e-prints, arXiv:1208.4012
- Griest, K., & Safizadeh, N. 1998, ApJ, 500, 37
- Han, C., & Gould, A. 1995, ApJ, 447, 53
- . 1996, ApJ, 467, 540
- Hwang, K.-H., Choi, J.-Y., Bond, I. A., et al. 2013, ApJ, 778, 55
- Janczak, J., Fukui, A., Dong, S., et al. 2010, ApJ, 711, 731
- Kervella, P., Thévenin, F., Di Folco, E., & Ségransan, D. 2004, A&A, 426, 297
- Kubas, D., Beaulieu, J. P., Bennett, D. P., et al. 2012, A&A, 540, A78
- Muraki, Y., Han, C., Bennett, D. P., et al. 2011, ApJ, 741, 22
- Penny, M. T., Kerins, E., Rattenbury, N., et al. 2013, MNRAS, 434, 2
- Penny, M., et al. 2014, in prep
- Poleski, R., Udalski, A., Gould, A., et al. 2013, ApJ, 776, 76
- Robin, A. C., Reylé, C., Derrière, S., & Picaud, S. 2003, A&A, 409, 523
- Sahu, K. C., Albrow, M., Anderson, J., et al. 2012, in American Astronomical Society Meeting Abstracts, Vol. 220, American Astronomical Society Meeting Abstracts #220, #307.03
- Spergel, D., Gehrels, N., Brekinridge, J., et al. 2013, ArXiv e-prints, arXiv:1305.5422
- Sumi, T., Kamiya, K., Bennett, D. P., et al. 2011, Nature, 473, 349
- Sumi, T., Bennett, D. P., Bond, I. A., et al. 2013, ApJ, 778, 150
- Walker, M. A. 1995, ApJ, 453, 37
- Yee, J. C. 2013, ApJ, 770, L31
- Yoo, J., DePoy, D. L., Gal-Yam, A., et al. 2004, ApJ, 603, 139
- Zhu, W. and Penny, M. and Mao, S., et al. 2014, ApJ, 788, 73